

Postannealing of coldly condensed Ag films: Influence of pyridine preadsorption

A. Humbert,* J. K. Gimzewski, and B. Reihl

IBM Zurich Research Laboratory, 8803 Rüschlikon, Switzerland

(Received 11 June 1985)

Scanning tunneling microscopy is used to demonstrate that pyridine adsorption at low temperature on coldly condensed Ag films results in trenchlike features after annealing to room temperature. These features are tentatively assigned to reshaped intercrystallite channels present before annealing.

The structure of thick silver films condensed onto a cold substrate ($T \leq 150$ K) under ultrahigh vacuum (UHV) conditions has attracted much experimental attention in recent years. The motivation was to explain the numerous optical and electronic properties of these films that are irreversibly lost upon annealing to room temperature.¹⁻⁷ Surface-enhanced Raman scattering (SERS) from adsorbed molecules is probably the most extensively studied of these properties. However, controversies still exist on its interpretation, particularly on the relative importance of electromagnetic versus chemical models of the enhancement, since the microscopic and atomic-scale roughness have not been quantified on these coldly condensed films.⁸

As all investigations have to be performed at low temperature, *in situ* measurements of the surface roughness by electron-microscopy techniques are difficult and have not yet been reported.

Fortunately, indirect information on the local surface structure has been gained using well-established surface techniques: ultraviolet photoemission spectroscopy (UPS),⁹⁻¹³ thermal desorption spectroscopy (TDS),^{10,14} and Raman experiments.^{15,16} The porosity of coldly deposited Ag films has thus been recently established by Albano and co-workers^{10,11} from a detailed study of xenon adsorption. This conclusion was corroborated independently¹² and supported by previous TDS experiments of adsorbed pyridine.¹⁴

To explain their observations, Albano and co-workers^{10,11} propose the following structure for coldly condensed Ag films kept at low temperature ($T < 250$ K): The films consist of columnar crystals of size 5–15 nm, separated by deep (~ 15 nm) intercrystallite gaps (pores) about 0.5–1.5 nm in width. Moreover, they assign the loss of SERS activity upon annealing to room temperature (RT) to the “annihilation of the pores in the range $170 \text{ K} \leq T \leq 250 \text{ K}$.”^{10,11} In a recent coadsorption experiment¹⁶ of Xe and pyridine on coldly condensed silver films, it could be shown that Xe prevents pyridine from entering the SERS active pores.

In a previous experiment,¹⁷ we applied the novel technique of scanning-tunneling microscopy (STM)¹⁸ to measure in real space and with subnanometer resolution the topography of room-temperature-condensed and coldly condensed postannealed Ag films prepared under UHV conditions. Taking advantage of the resolution of the STM, we have observed that annealing to RT of a coldly condensed Ag film ($T \sim 90$ K) on which pyridine was adsorbed at low temperature, results in a surface topography which can be related to the model proposed by Albano and co-workers^{10,11} for SERS-active surfaces, despite the fact that annealing causes a loss in SERS activity.³⁻⁶

In this Rapid Communication, we investigate in more de-

tail the role played by pyridine preadsorption, and show that it preserves features characteristic of SERS-active surfaces after annealing to RT.

All the samples investigated are thick (≥ 100 nm) Ag films condensed on polished Cu substrates in a UHV system built for inverse photoemission.¹⁹ Just prior to the rapid transfer of films through the air into the STM system, they are covered at RT with a thick layer of pyridine at an ambient pressure of nitrogen to minimize contamination. Subsequent Auger electron spectroscopy confirms only submonolayer contamination by C, S, O, and Cl. The STM pictures are recorded at RT in a vacuum of 10^{-8} mbar, which results in complete desorption of the pyridine.

Polycrystalline tungsten tips at voltages $V_t = +0.3$ to 0.6 V and tunnel currents $i_t = 1$ to 10 nA are used for the tunneling experiments. The images presented in Figs. 1–3 below were obtained direct on an X-Y recorder. Distortion owing to thermal and other drifts was checked and proved to be of insignificant importance. These images are representative of the different samples studied, and were selected from records taken on different areas of the same film and for different warmly and coldly condensed Ag films.

Figure 1 shows a typical STM picture for a film condensed at 100 K on which a thick layer of pyridine was adsorbed at low temperature prior to annealing at RT under UHV conditions. Columnar structures 5–15 nm in lateral extension, separated by trenchlike channels 1–3 nm in width, are clearly resolved. As discussed in our previous paper,¹⁷ the STM picture of the channels represents a convo-

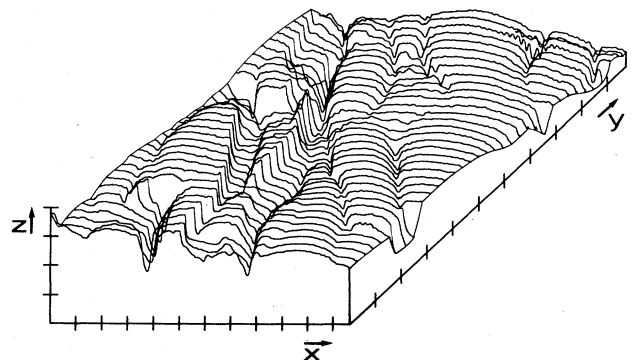


FIG. 1. An STM picture of a coldly condensed pyridine-treated Ag surface after annealing to 300 K. Division on the axes corresponds to 5 nm, after Ref. 17.

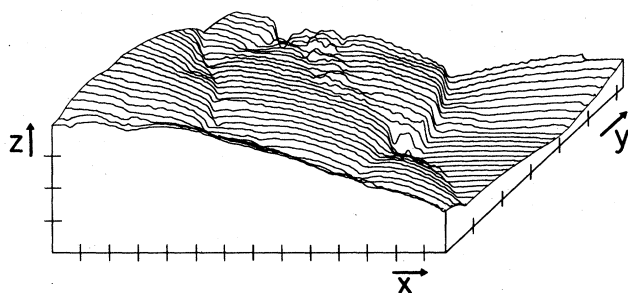


FIG. 2. An STM picture of a clean coldly condensed Ag surface after annealing to 300 K. Divisions on the axes correspond to 5 nm.

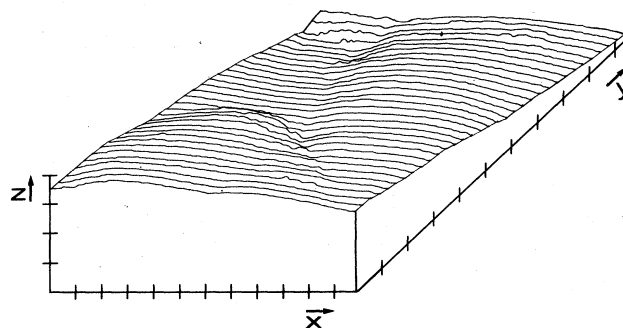


FIG. 3. An STM picture of an Ag surface condensed at 300 K. Divisions on the axes correspond to 5 nm.

lution of the channel and tip structure. The V-shaped features reflect predominantly the tip structure, and penetration of the tip into those sites is limited by tip geometry. In contrast, the bottom of some larger channels appear to be relatively flat, indicating that here the tip tunnels at the bottom of these channel sites. Consequently, an estimated lower limit of the channel depth lies between 3 and > 4.5 nm. Apart from the channel sites, the overall topography in Fig. 1 would be flat on the scale of the resolution limit of most scanning electron microscopes.

The absence of pyridine preadsorption results in an almost complete annihilation of the original intercrystallite channels, although occasionally isolated channels are observed: Figure 2 shows a typical STM picture for such a film condensed at 100 K and postannealed in UHV to RT. Postannealing of the film gives rise to compact grain boundaries and crystallites of about 5–20 nm in size. Comparison with Fig. 1 gives direct evidence for the role of pyridine preadsorption on channel retention during the annealing process.

Figure 3 shows a typical STM picture for a film con-

densed at RT. Compact grain boundaries are observed that connect crystallites of larger size (few hundred angstroms). Comparison with Fig. 2 shows that even in the absence of pyridine preadsorption, coldly condensed postannealed Ag films retain some memory of their previous porous structure.

Our results are consistent with photoemission data of adsorbed xenon reported by Albano and co-workers:^{10,11} The porous structure characteristic of coldly deposited thick Ag films almost disappears upon annealing to RT if these films are clean. However, our results demonstrate that pyridine preadsorption at low temperatures results in trenchlike features after annealing to RT. We tentatively assign these features to reshaped intercrystallite channels present before annealing.

We thank A. Baratoff for helpful discussions, and F. Rohner and R. Schlittler for technical assistance.

*On leave from CNRS, UA 783, Faculté des Sciences de Luminy, 13288 Marseille Cédex 9, France.

¹O. Hunderi and H. P. Myers, *J. Phys. F* **3**, 683 (1973).

²D. P. Dilella, R. H. Lipson, P. McBreen, and M. Moskovits, *J. Vac. Sci. Technol.* **18**, 453 (1981).

³A. Otto, I. Pockrand, J. Billman, and C. Pettenkofer, in *Surface Enhanced Raman Scattering*, edited by R. K. Chang and R. E. Furtak (Plenum, New York, 1982), p. 147.

⁴A. Otto, in *Light Scattering in Solids*, edited by M. Cardona and G. Güntherodt (Springer, Berlin, 1984), Vol. 4, p. 289.

⁵T. H. Wood, *Phys. Rev. B* **24**, 2289 (1981); **27**, 5137 (1983); T. H. Wood and M. V. Klein, *Solid State Commun.* **35**, 263 (1980).

⁶H. Seki, *Solid State Commun.* **42**, 695 (1982); *J. Chem. Phys.* **76**, 4412 (1982); *J. Vac. Sci. Technol.* **20**, 584 (1982); **18**, 633 (1981).

⁷T. Lopez-Rios, G. Vuye, and Y. Borensztein, *Surf. Sci.* **131**, L367 (1983).

⁸R. K. Chang, *J. Phys. (Paris) Colloq.* **44**, C10-283 (1983).

⁹J. Eickmans, A. Goldmann, and A. Otto, *Surf. Sci.* **127**, 153 (1983).

¹⁰E. V. Albano, S. Daiser, G. Ertl, R. Miranda, K. Wandelt, and N. Garcia, *Phys. Rev. Lett.* **51**, 2314 (1983).

¹¹E. V. Albano, S. Daiser, R. Miranda, and K. Wandelt, *Surf. Sci.* **150**, 367 (1985).

¹²J. Eickmans, A. Otto, and A. Goldmann, *Surf. Sci.* **149**, 293 (1984).

¹³C. Pettenkofer, J. Eickmans, Ü. Ertük, and A. Otto, *Surf. Sci.* **151**, 9 (1985).

¹⁴H. Seki and T. J. Chuang, *Chem. Phys. Lett.* **100**, 393 (1983).

¹⁵C. Pettenkofer, I. Pockrand, and A. Otto, *Surf. Sci.* **135**, 52 (1983).

¹⁶H. Seki, T. J. Chuang, M. R. Philpott, E. V. Albano, and K. Wandelt, *Phys. Rev. B* **31**, 5533 (1985).

¹⁷J. K. Gimzewski, A. Humbert, J. G. Bednorz, and B. Reihl, *Phys. Rev. Lett.* **55**, 951 (1985).

¹⁸G. Binnig, H. Rohrer, Ch. Gerber, and E. Weibel, *Phys. Rev. Lett.* **49**, 57 (1982); for a review and references, see G. Binnig and H. Rohrer, *Physica B* **127**, 37 (1984).

¹⁹B. Reihland and R. R. Schlittler, *Phys. Rev. B* **29**, 2267 (1984).